JPET Fast Forward. Published on May 28, 2015 as DOI: 10.1124/jpet.115.225631
This article has not been copyedited and formatted. The final version may differ from this version.

JPET #225631

Bioengineering novel chimeric microRNA-34a for prodrug cancer therapy: High-yield expression and purification, and structural and functional characterization

Wei-Peng Wang, Pui Yan Ho, Qiu-Xia Chen, Balasubrahmanyam Addepalli, Patrick A. Limbach, Mei-Mei Li, Wen-Juan Wu, Joseph L. Jilek, Jing-Xin Qiu, Hong-Jian Zhang, Tianhong Li, Theodore Wun, Ralph DeVere White, Kit S. Lam, Ai-Ming Yu

Department of Biochemistry & Molecular Medicine, School of Medicine, UC Davis, Sacramento, CA 95817, USA (W.-P. W., P.Y. H., Q.-X. C., M.-M. L., W.-J. W., J. L. J., K. S. L, A.-M. Y.); Center of Drug Metabolism and Pharmacokinetics, College of Pharmaceutical Sciences, Soochow University, Suzhou, Jiangsu 215123, China (W.-P, W, H.-J. Z); Rieveschl Laboratories for Mass Spectrometry, Department of Chemistry, University of Cincinnati, Cincinnati, OH 45221-0172, USA (B. A., P. A. L.); Department of Pathology, Roswell Park Cancer Institute, Buffalo, NY 14263, USA (J.-X. Q.); Division of Hematology Oncology, School of Medicine, UC Davis, Sacramento, CA 95817, USA (T. L., T. W. K. S. L); Department of Urology, School of Medicine, UC Davis, Sacramento, CA 95817, USA (R. D.-V. W).

Running title: Biologic miR-34a as anticancer prodrug

Address correspondence to: Prof. Ai-Ming Yu, Department of Biochemistry & Molecular Medicine, UC Davis School of Medicine, 2700 Stockton Blvd., Suite 2132, Sacramento, CA 95817; Tel: +1 916-734-1566; Fax: +1 916-734-4418; Email: aimyu@ucdavis.edu.

Number of Text Pages: 23

Number of Figures: 7

Number of References: 42

Number of Words in Abstract: 250

Number of Words in Introduction: 957

Number of Words in Discussion: 1356

Abbreviations: miR or miRNA, microRNA; miR-34a, microRNA-34a; pre-miR-34a or mir-34a, pre-microRNA-34a; ncRNA, noncoding RNA; tRNA/mir-34a, tRNA fusion pre-miR-34a; *E. coli*, *Escherichia coli*; tRNA, transfer RNA; CDK6, cyclin-dependent kinase 6; MET, hepatocyte growth factor receptor; SIRT1, sirtuin-1; FPLC, past protein liquid chromatography; LC-UV-MS, liquid chromatography coupled with ultraviolet and mass spectrometry detection; LC-MS/MS, liquid chromatography-tandem mass spectroscopy; PAGE, polyacrylamide gel electrophoresis; RT-qPCR, reverse transcription quantitative real-time polymerase chain reaction.

JPET Fast Forward. Published on May 28, 2015 as DOI: 10.1124/jpet.115.225631
This article has not been copyedited and formatted. The final version may differ from this version.

Abstract

Development of microRNA (miRNA or miR) based treatments such as miR-34a replacement therapy is limited to the use of synthetic RNAs with artificial modifications. Herein we present a new approach to high-yield and large-scale biosynthesis of chimeric miR-34a agent in *Escherichia coli* using tRNA scaffold, which may act as a prodrug for cancer therapy. The recombinant tRNA fusion pre-miR-34a (tRNA/mir-34a) was quickly purified to a high degree of homogeneity (> 98%) using anion-exchange fast protein liquid chromatography (FPLC), whose primary sequence and posttranscriptional modifications were directly characterized by mass spectrometric analyses. Chimeric tRNA/mir-34a showed favorable cellular stability while it was degradable by several ribonucleases. Deep sequencing and qPCR studies revealed that tRNA-carried pre-miR-34a was precisely processed to mature miR-34a within human carcinoma cells, whereas the same tRNA fragments were produced from tRNA/mir-34a and the control tRNA scaffold (tRNA/MSA). Consequently, tRNA/mir-34a inhibited the proliferation of varoius types of human carcinoma cells in a dose dependent manner and to much greater degrees than the control tRNA/MSA, which was mechanistically attributable to the reduction of miR-34a target genes. Furthermore, tRNA/mir-34a significantly suppressed the growth of human non-small cell lung cancer A549 and hepatocarcinoma HepG2 xenograft tumors in mice, compared to the same dose of tRNA/MSA. In addition, recombinant tRNA/mir-34a had no or minimal effects on blood chemistries and IL-6 levels in mouse models, suggesting that recombinant RNAs were well tolerated. These findings provoke a conversation on producing biological miRNAs to perform miRNA actions, and point towards a new direction to develop miRNA-based therapies.

JPET Fast Forward. Published on May 28, 2015 as DOI: 10.1124/jpet.115.225631
This article has not been copyedited and formatted. The final version may differ from this version.

Introduction

MicroRNAs have been revealed as a large family of genomically-encoded noncoding RNAs (ncRNAs) that are critical factors in the control of cancer cell proliferation, apoptosis and invasion, and tumor initiation and progression (Kasinski and Slack, 2011; Bader, 2012), as well as drug disposition (Yu, 2009; Ingelman-Sundberg et al., 2013) and pathogenesis of other diseases (Yao and Li, 2015). Research on miRNA biological functions has offered clues to develop novel cancer treatments, and a number of miRNA-based therapies are indeed under or moving towards clinical trials. In particular, oncogenic miRNAs such as miR-10b, which are upregulated in cancer cells, may be targeted to achieve the control of cancer cell proliferation and tumor growth (Ma et al., 2007). On the other hand, tumor suppressive miRNAs such as miR-34a showing a loss-of-function in cancerous tissues may be reintroduced into cancer cells to suppress tumor progression (He et al., 2007; Welch et al., 2007). The later approach, namely "miRNA replacement therapy", is distinguished from the former miRNA antagonism strategy. The miRNA or pre-miRNAs used in miRNA replacement therapy have the same sequences as genomically-encoded miRNAs or pre-miRNAs, and therefore unlikely to produce "off-target" effects. Meanwhile, because miRNAs are normal constituents of healthy cells, reintroduction of therapeutic miRNAs is unlikely to cause major toxicity (Bader, 2012).

Human miR-34a is one of the most promising tumor suppressive miRNAs for cancer treatment. Loss of miR-34a expression has been documented in a wide range of solid tumors and hematological malignancies, including lung, prostate, breast, pancreas, liver, colon, kidney, bladder, skin, esophagus, brain, cervix, ovary, urothelium and lymphoid systems (see review (Bader, 2012)). While the biogenesis of miR-34a is directly controlled by tumor protein p53 at the transcriptional level (Chang et al., 2007; He et al., 2007), ectopic expression of miR-34a leads to a dramatic reprogramming of a set of target genes such as cyclin-dependent kinase 6 (CDK6), hepatocyte growth factor receptor MET, platelet-derived growth factor receptor-alpha (*PDGFRA*) and GTPase KRAS, and consequently inhibits cancer cell proliferation, induces cell cycle arrest and enhances apoptosis (Chang et al., 2007; He et al., 2007; Sun et al., 2008; Yamakuchi et al., 2008; Li et al., 2009; Kasinski and Slack, 2012). Meanwhile, miR-34a can stimulate endogenous p53 activity in a positive feedback-loop by targeting the NAD-dependent

deacetylase sirtuin-1 (SIRT1) that deactivates p53, and the transcriptional repressor Yin Yang 1 (YY1) that binds to p53 and promotes p53 ubiquitination and degradation (Yamakuchi et al., 2008). Moreover, miR-34a suppresses clonogenic expansion, tumor regeneration and metastasis through targeting CD44 and cancer stem cells or tumor-initiating cells (Liu et al., 2011). The anticancer activity of miR-34a has been nicely demonstrated in various types of human carcinoma cells *in vitro* including lung, liver, pancreas, colon, brain, skin, prostate, bone, ovary, as well as lymphoma and leukemia. In addition, although the performance of miR-34a replacement therapy in animal models depends heavily on the delivery system used, a number of successful examples have illustrated the effectiveness of miR-34a in inhibiting progression of many types of xenograft tumors, including non-small cell lung cancer (Wiggins et al., 2010; Kasinski and Slack, 2012), prostate cancer (Liu et al., 2011), pancreatic cancer (Pramanik et al., 2011) and lymphomas (Craig et al., 2012). As a result, "MRX34", a liposome-formulated miR-34a, has entered Phase I clinical trials for the treatment of unresectable primary liver cancer (Kelnar et al., 2014).

Nevertheless, research on miRNA pharmacology and therapeutics rely primarily on the use of synthetic RNAs (e.g., miRNA mimics and antagomirs, and pre-miRNAs (mir)) and recombinant DNA agents (e.g., viral or non-viral vector-based miRNA or "decoy" antisense RNA expression plasmids). The use of DNA materials may complicate the RNA-based processes, and this approach also relies on the host cells or organisms to transcribe the gene to miRNA precursors before the generation of mature miRNAs. Despite that organic synthesis of oligonucleotides may be automated, a multi-milligram dose of 22-nt double-stranded miRNA mimics projected for *in-vivo* testing or therapy is very costly. In addition, it is unknown how artificial modifications may alter the folding, biological activities and safety profiles, even though synthetic miRNAs exhibit some favorable pharmacokinetic properties such as a longer half-life.

Motivated by the idea to deploy biological RNAs to perform RNA actions for pharmacotherapy, we aimed to bioengineer pre-miRNA (mir) agents in common strains of bacteria on a large scale using the tRNA scaffold (Ponchon and Dardel, 2007; Ponchon et al., 2009; Nelissen et al., 2012). We hypothesized that the tRNA fusion pre-miRNA (tRNA/mir) could act as a prodrug where pre-miRNA might be selectively processed to mature miRNA in human cells, and tRNA scaffold

would be metabolized or degraded to tRNA fragments (tRFs). In contrast to a low-yield production of pre-miR-27b (Li et al., 2014), we present herein an optimal expression and rapid purification of multi-milligrams of tRNA fusion pre-miR-34a (tRNA/mir-34a) from 1 L bacterial culture in a research laboratory setting. The molecular weight, primary sequence, and posttranscriptional modifications of recombinant tRNA/mir-34a were directly characterized by mass spectrometry (MS) studies. Furthermore, unbiased deep sequencing study and targeted qPCR analyses showed that tRNA-carried pre-miR-34a was indeed processed precisely into mature miR-34a in human carcinoma cells, leading to a 70- to 100-fold increase in cellular miR-34a levels. Consequently, tRNA/mir-34a significantly suppressed the protein levels of miR-34a target genes (e.g., CDK6, SIRT1, and MET) and proliferation of human lung (A549 and H460) and liver (HepG2 and Huh-7) cancer cells *in vitro* in a dose-dependent manner, as compared to the control tRNA scaffold (tRNA/MSA). In addition, we demonstrated that recombinant tRNA/mir-34a was well tolerated in animal models, and remarkably repressed A549 and HepG2 xenograft tumor growth *in vivo*. These findings indicate that biological RNA agents engineered in bacteria may serve as a new category of RNA agents for drug discovery as well as basic and translational research.

JPET Fast Forward. Published on May 28, 2015 as DOI: 10.1124/jpet.115.225631
This article has not been copyedited and formatted. The final version may differ from this version.

Materials and Methods

Chemicals and Materials. Lipofectamine 2000, Trizol reagent and BCA Protein Assay Kit were purchased from Thermo Fisher Scientific Inc. (Waltham, MA). RIPA lysis buffer was bought from Rockland Immunochemicals (Limerick, PA), and the complete protease inhibitor cocktail was purchased from Roche Diagnostics (Mannheim, Germany). The antibodies against CDK6 (C-21), SIRT1 (H-300), Met (C-28) and glyceraldehyde-3-phosphate dehydrogenase (GAPDH) were purchased from Santa Cruz Biotech Inc. (Texas, TX), and peroxidase goat anti-rabbit IgG was from Jackson ImmunoResearch Inc. (West Grove, PA). ECL substrate and PVDF membrane were bought from Bio-Rad (Hercules, CA). All other chemicals and organic solvents of analytical grade were purchased from Sigma-Aldrich (St. Louis, MO) or Thermo Fisher Scientific Inc. (Waltham, MA).

Bacterial Culture. All *E. coli* stains were cultured at 37°C in LB broth supplemented with 100 μg/mL ampicillin. DH5α and TOP10 (Life Technologies, Grand Island, NY) were used for cloning as well as screening for recombinant ncRNA expression. BL21 (Sigma-Aldrich, St. Louis, MO) and HST08 (Clontech Laboratories, Mountain View, CA) were also used to screen ncRNA accumulation. HST08 was identified and utilized for large-scale production of recombinant ncRNAs.

Human Cell Culture. The human carcinoma cell lines HepG2, Huh-7, A549 and H460 were purchased from American Type Culture Collection (Manassas, VA). HepG2 cells were cultured in EMEM medium, A549 and H460 cells in RPMI 1640 medium, and Huh-7 cells in DMEM medium supplemented with 10% fetal bovine serum (GBICO BRL, Rockville, MD), at 37°C in a humidified atmosphere containing 5% CO_2. Cells in the logarithmic growth phase were used for experiments.

Prediction of RNA Secondary Structure. The secondary structures of various sizes of human pre-miR-34a, tRNA scaffold, and the chimeric ncRNAs were predicted using the CentroidFold (http://www.ncrna.org/centroidfold), CentroidHomfold (http://www.ncrna.org/centroidhomfold),

JPET Fast Forward. Published on May 28, 2015 as DOI: 10.1124/jpet.115.225631
This article has not been copyedited and formatted. The final version may differ from this version.

and RNAstructure (http://rna.urmc.rochester.edu/RNAstructureWeb/Servers/Predict1/Predict1.html).

Construction of tRNA/mir-34a Expression Plasmids. The DNA fragments encoding 112-nt and 129-nt human pre-miR-34a (miRBase ID: MI0000268) were amplified from human genomic DNA by PCR using the primers 5'-AGT AAT TTA CGT CGA CGG CCA GCT GTG AGT GTT TCT TTG G-3' and 5'-CGG CCG CAA CCA TCG ACG TCT GGG CCC CAC AAC GTG CAG CAC TT-3', and 5'-AGT AAT TTA CGT CGA CGT GGA CCG GCC AGC TGT GAG TGT T-3' and 5'-CGG CCG CAA CCA TCG ACG TCA TCT TCC CTC TTG GGC CCC ACA ACG-3' (IDT, San Diego, CA), respectively. The amplicons were inserted into the pBSMrnaSeph vector (kindly provided by Dr. Luc Ponchon at the Université Paris Descartes) (Ponchon et al., 2009) linearized with *Sal*I-HF® and *Aat*II (New England Biolabs, Ipswich, MA). Target tRNA/mir-34a expression plasmids were confirmed by Sanger sequencing analyses at UC Davis Genome Center.

Expression of Recombinant ncRNAs in *E. coli*. Recombinant ncRNAs were expressed in HST08 as described (Ponchon and Dardel, 2007; Ponchon et al., 2009; Li et al., 2014). Total RNAs were isolated using the Tris-HCl-saturated phenol extraction method, quantitated with a NanoDrop 2000 spectrophotometer (Thermo Fisher Scientific, Rockford, IL), and analyzed by denaturing urea (8 M) polyacrylamide (8%) gel electrophoresis (PAGE) to assess the expression of recombinant ncRNAs. We usually loaded 0.2-1.0 μg RNAs per lane for the urea-PAGE analysis. The ssRNA ladder and siRNA marker were purchased from New England Biolabs. Images were acquired with ChemiDo MP Imaging System (Bio-Rad, Hercules, CA), and intensities of bands were used to provide a rough estimation of relative levels of recombinant ncRNAs present in the total RNAs.

Affinity Purification of Recombinant ncRNAs. Purification of sephadex aptamer-tagged ncRNAs using Sephadex G-100 beads (Sigma-Aldrich) was conducted as reported (Ponchon et al., 2009; Li et al., 2015), and RNA fractions were analyzed by urea-PAGE.

JPET Fast Forward. Published on May 28, 2015 as DOI: 10.1124/jpet.115.225631
This article has not been copyedited and formatted. The final version may differ from this version.

FPLC Purification of Recombinant ncRNAs. Recombinant tRNA/mir-34a was purified from total RNAs on a UNO Q6 anion-exchange column (Bio-Rad) using a NGC QUEST 10PLUS CHROM FPLC System (Bio-Rad). After the samples were loaded, the column was first equilibrated with Buffer A (10 mM sodium phosphate, pH = 7.0) at a flow rate 6.0 mL/min for 0.5 min, followed by a gradient elution at the same flow rate, 0-56% Buffer B (Buffer A plus 1 M sodium chloride) in 0.5 min, 56% Buffer B for 2 min, 56-65% Buffer B in 10 min, and then 100% Buffer B for 2 min, 100-0% Buffer B in 0.5 min and 100% Buffer A for 5 min. The salt gradient elution condition for the control tRNA/MSA was essentially the same as reported (Li et al., 2014). FPLC traces were monitored at 260 nm using a UV/Vis detector. Peak areas were also utilized to estimate the relative levels of recombinant ncRNAs within the total RNAs, which were consistent with those determined by urea-PAGE analyses. After analyzed by urea-PAGE, the fractions containing pure ncRNAs were pooled. Recombinant ncRNAs were precipitated with ethanol, reconstituted with nuclease-free water, and then desalted and concentrated with Amicon ultra-2 mL centrifugal filters (30 KD; EMD Millipore, Billerica, MA). The quantity of ncRNAs was determined using a NanoDrop 2000 spectrophotometer and the quality was validated by PAGE and HPLC analysis before other experiments.

HPLC Analysis of Purified ncRNAs. HPLC analysis was conducted using an XBridge OST C_{18} column (2.1 × 50 mm, 2.5 μm particle size; Waters, Milford, MA) on a Shimadzu LC-20AD HPLC system. The flow rate was 0.2 mL/min, and the column was maintained at 60 °C. Mobile phase A consisted of 8.6 mM triethylamine (TEA) and 100 mM hexafluoroisopropanol (HFIP, pH 8.3) in water, and mobile phase B consisted of 8.6 mM TEA and 100 mM HFIP in methanol. The LC gradient was as follows: 0-1 min, 16% mobile phase B; 21 min, 22% mobile phase B. RNA was monitored at 260 nm using a photodiode array detector.

Removal and Detection of Endotoxin. Endotoxin was further removed from FPLC-purified ncRNAs using the CleanAll DNA/RNA Clean-up Kit (Norgen Biotek, Thorold, ON, Canada) and Endotoxin-free Water (Lonza, Walkersville, MD), as instructed by the manufacturer. Endotoxin activities in total RNAs as well as the FPLC-purified and CleanAll Kit-processed ncRNA samples were determined using the Pyrogent-5000 kinetic LAL assay (Lonza) by following the instructions. In particular, a SpectraMax3 plate reader (Molecular Devices,

Sunnyvale, CA) was used to measure turbidity at a 340 nm wavelength. Provided endotoxin standards were used to generate a standard curve, and endotoxin levels in RNA samples were expressed in EU/μg RNA (endotoxin units/μg RNA).

Electrospray Ionization-Mass Spectrometry (ESI-MS) Analysis of Intact Recombinant ncRNAs. The procedures described by Taucher and Breuker (Taucher and Breuker, 2010) were followed. The instrumental settings were optimized by automatic tuning with poly $d(T)_{80}$. The mass spectra were acquired in negative ion mode using a Thermo LTQ XL-ion trap mass spectrometer over an *m/z* range of 600–2000. ESI mass spectra of intact ncRNAs were deconvoluted using ProMass software for Xcalibur (Version 2.8 rev. 2) (Novatia LLC, Newtown, PA) to determine the average molecular weights (MWs) of recombinant RNAs.

Nucleoside Analysis by LC-UV-MS. The hydrolysates were prepared with Nuclease P1 (Sigma-Aldrich), snake venom phosphodiesterase (Worthington Biochemicals Lakewood, Lakewood, NJ) and antarctic phosphatase (New England Biolabs), resolved on a 5 μm, 2.1 mm × 250 mm Supelcosil LC-18-S column using a Hitachi D-7000 HPLC system, and analyzed by a diode array detector and a Thermo LTQ-XL ion trap mass spectrometer, as described by Russell and Limbach (Russell and Limbach, 2013).

RNA Mapping by LC-MS/MS. RNA mapping and assignment of modifications using a Thermo Surveyor HPLC system coupled to a Thermo LTQ XL ion trap mass spectrometer and a Thermo Micro AS autosampler after the digestion with RNase T1 (Roche Molecular Biochemicals, Indianapolis, IN) and bacterial alkaline phosphatase (Worthington Biochemical Corporation) was carried out as described (Krivos et al., 2011). Collision-induced dissociation tandem mass spectrometry (CID MS/MS) was used to obtain sequence information from the RNase digestion products.

Susceptibility to RNases. Recombinant ncRNAs were digested by individual RNases in provided buffer or HEPES (100 mM KCl, 5 mM $MgCl_2$, 10 mM HEPES, pH 7.4) at 37°C for 1 h. In particular, 12 μg ncRNAs were incubated with 1 μg/mL human recombinant RNase I (Novoprotein, Summit, NJ), 12 μg ncRNAs with 10 μg/mL Human Recombinant Angiogenin

JPET Fast Forward. Published on May 28, 2015 as DOI: 10.1124/jpet.115.225631
This article has not been copyedited and formatted. The final version may differ from this version.

(R&D Systems, Minneapolis, MN), 1 μg ncRNAs with 1 U of recombinant Dicer (Genlantis Inc., San Diego, CA), 6 μg ncRNAs with 5 U of bacterial RNase III (Life Technologies), and 5 μg ncRNAs with 5 U of RNase R (Epicentre, Madison, WI). Likewise, 4 μg RNA was formulated with 0.64 μL *in vivo*-jetPEI (Polyplus-transfection Inc., New York, NY) delivery agent to a 5% final glucose concentration, and then added to OptiMEM with or without 1 μL human serum (Thermo Scientific) to a 100 μL volume and incubated at 37°C for 20 min. The digestion products were analyzed by 8% urea PAGE.

Reverse Transcription Quantitative Real-Time PCR (RT-qPCR). Total RNA was isolated from cells using Direct-zol RNA MiniPrep kit (Zymo Research, Irvine, CA), and reverse transcribed with NxGen M-MuLV reverse transcriptase (Lucigen, Middleton, WI) and stem-loop primer 5'-GTC GTA TCC AGT GCA GGG TCC GAG GTA TTC GCA CTG GAT ACG ACA CAA CC-3' for miR-34a, or iScript reverse-transcription Supermix (Bio-Rad) for chimeric ncRNAs, pre-miR-34a and U6. Quantitative real-time PCR (qPCR) was conducted with quantitative RT-PCR Master mix (New England Biolabs) on a CFX96 Touch real-time PCR system (Bio-Rad), as described (Bi et al., 2014; Li et al., 2014). The primers were as follows: 5'-GGC TAC GTA GCT CAG TTG GT-3' (forward) and 5'-TGG TGG CTA CGA CGG GAT TC-3' (reverse) for chimeric ncRNAs; 5'-GGC CAG CTG TGA GTG TTT CTT TGG-3' (forward) and 5'-GGG CCC CAC AAC GTG CAG-3' (reverse) for pre-miRNA mir-34a; 5'-CGC GCT GGC AGT GTC TTA GCT-3' (forward) and 5'-GTG CAG GGT CCG AGG T-3' (reverse) for mature miR-34a; and 5'-CTC GCT TCG GCA GCA CA-3' (forward) and 5'-AAC GCT TCA CGA ATT TGC GT-3' (reverse) for U6. The relative expression was calculated by using the comparative threshold cycle (Ct) method with the formula $2^{-\Delta\Delta Ct}$.

Small RNA Library Construction. Total RNAs were isolated with Trizol reagent (Invitrogen) from A549 cells harvested at 48 h post-treatment with highly purified ncRNAs or Lipofectamine 2000 (Life Technologies) itself, and the small RNA library was generated using the Illumina Truseq™ Small RNA Preparation kit (Illumina, San Diego, CA) according to the instructions.

Deep Sequencing and Data Analysis. The purified cDNA library was used for cluster generation on Illumina's Cluster Station and then sequenced on Illumina GAIIx following

vendor's instructions. Raw sequencing reads (40 nt) were obtained using Illumina's Sequencing Control Studio software version 2.8 (SCS v2.8) following real-time sequencing image analysis and base-calling by Illumina's Real-Time Analysis version 1.8.70 (RTA v1.8.70). The extracted sequencing reads were used for the standard sequencing data analysis by following a proprietary pipeline script, ACGT101-miR v4.2 (LC Sciences, Houston, TX).

Immunoblot Analysis. The cell lysates were prepared using RIPA buffer (Rockland Immunochemical Inc., Limerick, PA) supplemented with the complete protease inhibitor cocktail (Roche, Nutley, NJ). Protein concentrations were determined using the BCA Protein Assay Kit (Thermo Fisher Scientific). Proteins were separated on a 10% SDS-PAGE gel and electro-transferred onto PVDF membranes using Trans-Blot Turbo Transfer System (Bio-Rad). Membranes were incubated with CDK6 (C-21), SIRT1 (H-300), or Met (C-28) rabbit polyclonal antibody (Santa Cruz Biotech Inc., Texas, TX) and subsequently with a peroxidase goat anti-rabbit IgG (Jackson ImmunoResearch Inc., West Grove, PA). The membranes were then incubated with Clarity Western ECL substrates (Bio-Rad) and visualized with the ChemiDoc MP Imaging System (Bio-Rad).

Cytotoxicity. The effects of tRNA/mir-34a on the proliferation of cancer cells were determined using an MTT assay, as described (Pan et al., 2013; Li et al., 2015). Cells were seeded in 96-well plates at 3,000 or 5,000 cells per well, and transfected with various concentrations of tRNA/mir-34a using Lipofectamine 2000 for 72 h. Cells transfected with the same doses of tRNA/MSA or Lipofectamine 2000 were used as controls. The EC50 and Hill slope values were estimated by fitting the data to a normalized inhibitory dose-response model (GraphPad Prism, San Diego, CA).

Xenograft Tumor Mouse Models. All animal procedures were approved by the Institutional Animal Care and Use Committee at UC Davis. A549 and HepG2 cells were collected, counted, and mixed with Matrigel (BD Biosciences, San Jose, CA) in a 1:1 ratio by volume. Cells (5×10^6) in 100 μL of medium/Matrigel solution were injected s.c. into the lower back region of 5- to 6-week-old male nude mice (The Jackson Laboratory, Bar Harbor, ME). Tumor volumes were measured with a caliper and calculated according to the formula, tumor volume (mm^3) = 0.5 ×

JPET Fast Forward. Published on May 28, 2015 as DOI: 10.1124/jpet.115.225631
This article has not been copyedited and formatted. The final version may differ from this version.

(length (mm) × width^2 (mm^2)). Recombinant tRNA/mir-34a and control tRNA/MSA were formulated with *in vivo*-jetPEI (Polyplus-transfection Inc.) and administered intratumorally (i.t.) once tumors reached 150-200 mm^3. Tumors were collected, fixed in 10% formalin and cut for histological verification by pathologist.

Safety Profiles in Mouse Models. Male BALB/c mice at five to six weeks of age (The Jackson Laboratory) were administered i.v. via tail vein with 100 μg of ncRNAs formulated with *in vivo*-jetPEI. Separate groups of animals were treated with *in vivo*-jetPEI vehicle as a negative control or 20 μg of lipopolysaccharide (LPS) as a positive control for cytokine induction (Wiggins et al., 2010; Bodeman et al., 2013; Wang et al., 2015). Blood was collected at various time points and serum was isolated using the serum separator (BD Biosciences). Serum cytokine IL-6 levels were quantitated using a mouse IL-6 assay kit (Pierce Thermo Scientific) on a SpectraMax M3 Multi-Mode Spectrophotometer (Molecular Devices), and mouse blood chemistry profiles were determined at the Comparative Pathology Laboratory at UC Davis.

Statistical Analysis. All data were presented as mean ± SD. According to the number of groups and variances, data were analyzed with unpaired Student's *t*-test, or one-way or two-way ANOVA (GraphPad Prism). Any difference was considered as significant if the probability was less than 0.05 ($P < 0.05$).

JPET Fast Forward. Published on May 28, 2015 as DOI: 10.1124/jpet.115.225631
This article has not been copyedited and formatted. The final version may differ from this version.

Results

Chimeric tRNA/mir-34a can be efficiently biosynthesized in a common strain of *E. coli* on a large scale and rapidly purified to a high degree of homogeneity. To achieve high-yield production of pre-miR-34a agents in *E. coli*, we chose to use the tRNA scaffold (Ponchon and Dardel, 2007; Ponchon et al., 2009) to assemble a fusion ncRNA namely tRNA/mir-34a (Figure 1A). The secondary structures predicted by different computational algorithms all indicated that the stem-loop structure of pre-miR-34a consisting of Dicer cleavage sites would be retained within tRNA/mir-34a chimeras. Thus the pre-miR-34a coding sequences were cloned to offer tRNA/mir-34a expression plasmids. Our data showed that slight change in the length of pre-miR-34a did not alter the levels of recombinant tRNA/mir-34a accumulated (Supplementary Figure S1A). Target tRNA/mir-34a agents were expressed in different common *E. coli* strains and the highest accumulation levels were found in HST08 cells (Figure 1B) at 9-14 h post-transformation (Supplementary Figure S1B). In addition, use of HST08 competent cells prepared within our laboratory offered similar levels of recombinant tRNA/mir-34a (Supplementary Figure S1C), and the high-level expression (e.g., ~15% of recombinant ncRNAs in total RNAs) was retained when bacterial cultures were scaled up to 0.5 L, and different batches of cultures were carried out (Supplementary Figure S1D), demonstrating a consistent and efficient expression of biological tRNA/mir-34a agents.

Next, we aimed to purify the recombinant tRNA/mir-34a to a high degree of homogeneity (e.g., >98%). Affinity purification was originally carried out for tRNA/mir-34a and the control tRNA/MSA bearing a Sephadex aptamer tag. Although affinity chromatography offered a good purity (> 90%), overall yield was not very satisfactory (around 2% of recombinant ncRNA/total RNAs) which may be attributed to an unexpected but obvious inefficient binding (Supplementary Figure S1E). Thus we developed an anion exchange FPLC method for the isolation of tRNA/mir-34a and tRNA/MSA from total RNAs using a salt gradient elution. This FPLC method not only enabled rapid isolation of target ncRNAs (< 25 min per run; Figure 1C) to a high degree of homogeneity (e.g., >98% purity, as demonstrated by gel electrophoresis (not shown) and HPLC analysis (Figure 1D) but also offered much higher purification yield (e.g., 67% according to the 15% target ncRNA present in total RNAs, or 10% recombinant ncRNA/total

JPET Fast Forward. Published on May 28, 2015 as DOI: 10.1124/jpet.115.225631
This article has not been copyedited and formatted. The final version may differ from this version.

RNAs loaded on column). This FPLC method largely facilitated the purification process which allows us to readily obtain milligrams of ncRNAs, i.e., ~1.5 mg of >98% pure tRNA/mir-34a from 15 mg of total RNAs isolated from 0.5 L bacterial culture at all times.

Recombinant ncRNAs carry posttranscriptional modifications. To delineate if the recombinant tRNA/mir-34a are comprised of any posttranscriptional modifications, which are common for natural RNAs produced in living cells (Novoa et al., 2012), we employed several mass spectrometry-based techniques to analyze the purified ncRNAs after confirming their primary sequences by Sanger sequencing of reversely-transcribed cDNAs (data not shown). First, we determined the molecular weights (MWs) through electrospray ionization mass spectrometry (ESI-MS) analyses of the intact ncRNAs, which were 73,422.4 Da for tRNA/mir-34a and 34,765.2 Da for tRNA/MSA. The differences between the measured and predicted MWs (146.8 Da for tRNA/mir-34a, and 149.2 Da for tRNA/MSA; Supplementary Figure S2A) suggest the presence of modified nucleosides. We then conducted a LC-UV-MS analysis of ncRNA hydrolysates and identified a number of modified nucleosides for the tRNA scaffold (existing in both tRNA/mir-34a and tRNA/MSA), such as dihydrouridine (D), pseudouridine (ψ), 7-methylguanosine (m^7G), 4-thiouridine (s^4U), 2'-*O*-methylguanosine (Gm) and 3-(3-amino-3-carboxypropyl)uridine (acp^3U) (Supplementary Figure S2B). We thus carried out LC-MS/MS analyses (Supplementary Figure S2C) of RNA fragments produced from recombinant ncRNAs by RNase T1, which allowed us to successfully map the ncRNA sequences and localize all modified nucleosides for the tRNA scaffold (Figure 1E). The deoxyadenosine (dA) found in tRNA/mir-34a hydrolysates (Supplementary Figure S2B) was not mapped to its RNase T1 digestions, which might be attributable to prior carry-over or co-purified nucleic acid. Together, these data indicate that recombinant ncRNAs obtained from *E. coli* indeed consist of various posttranscriptional modifications that may be critical for RNA folding and metabolic stability.

tRNA-carried pre-miR-34a is selectively processed to mature miR-34a in human carcinoma cells while the tRNA scaffold is degraded to tRNA fragments. To assess whether chimeric tRNA/mir-34a can be selectively processed to mature miR-34a in human cells, we first conducted unbiased deep sequencing study. The RNAseq data revealed that the tRNA/mir-34a chimera was precisely processed to mature miR-34a in A549 cells, leading to a 70-fold increase

JPET Fast Forward. Published on May 28, 2015 as DOI: 10.1124/jpet.115.225631
This article has not been copyedited and formatted. The final version may differ from this version.

in miR-34a levels than the cells treated with tRNA/MSA or vehicle (Figure 2A-B). In contrast, there was no or limited changes in other cellular miRNAs, except a few undefined small RNAs (e.g., hsa-miR-30c-5p_R+1 and hsa-mir-7641-1-p5_1ss6TC, etc.; Figure 2A-B and Supplementary Tables S1-2) which might be secondary effects that were caused by the changes in miR-34a target gene expression (see the results below). Furthermore, the increase in miR-34a levels was attributed to the 22- and 23-nt isoforms that arose in tRNA/mir-34a-, tRNA/MSA- and vehicle-treated cells (Supplementary Table S3). In addition, the common tRNA scaffold was degraded in the cells to offer the same tRFs that exhibited similar patterns between tRNA/mir-34a- and tRNA/MSA-treated cells, whereas at much lower levels than mature miR-34a (Figure 2B; Supplementary Table S4), supporting the use of tRNA/MSA as a proper control to distinguish the activities of pre-miR-34a.

Recombinant tRNA/mir-34a exhibits a favorable cellular stability and is degradable by human RNases. Consistent with deep sequencing data, selective stem-loop RT-qPCR analyses revealed a 70- to 100-fold increase in mature miR-34a levels in human lung (A549 and H460) and liver (HepG2 and Huh-7) carcinoma cells after the transfection with tRNA/mir-34a (Figure 3A). Moreover, mature miR-34a and pre-miR-34a levels were elevated in tRNA/mir-34a-treated A549 cells in a dose dependent manner; whereas there was no change of miR-34a levels in cells treated with tRNA/MSA where tRNA/MSA levels were actually increased (Figure 3B). Most importantly, a high level of recombinant tRNA/mir-34a and tRNA/MSA persisted for 6 days in the cells post-transfection with levels gradually decreasing from day 3 (Figure 3C), indicating a favorable cellular stability. In addition, the change of pre-miR-34a and mature miR-34a levels over time were solely dependent upon the tRNA/mir-34a treatment. Further biochemical experiments demonstrated that tRNA/mir-34a and tRNA/MSA were readily processed by RNase A (or RNase I, the major form of ribonuclease in human serum) and Dicer (RNase III) but to a relatively lower degree by angiogenin (RNase 5) (Figure 3D), suggesting their involvement in the processing and degradation of recombinant ncRNAs. In contrast, bacterial RNase R was unable to cleave chimeric ncRNAs (data not shown), providing a good explanation for why such ncRNAs were accumulated to high levels within bacteria.

JPET Fast Forward. Published on May 28, 2015 as DOI: 10.1124/jpet.115.225631
This article has not been copyedited and formatted. The final version may differ from this version.

tRNA-carried pre-miR-34a is active to reduce miR-34a target gene expression and to inhibit cancer cell proliferation, equally or more effective than synthetic miR-34a agents. We thus assessed the efficacy of tRNA-carried pre-miR-34a in the control of miR-34a target gene expression and cancer cell growth, using tRNA/MSA as a critical control. Recombinant tRNA/mir-34a showed a dose dependent inhibition against the proliferation of all types of cancer cells tested in our studies, to a much greater degree than the control tRNA/MSA (Figure 4A and Supplementary Figure S3). The higher efficacy in suppressing cancer cell growth by tRNA/mir-34a was also indicated by the estimated EC50 values (Table 1). Inhibition of A549 and HepG2 carcinoma cell proliferation by tRNA/mir-34a was associated with a remarkable repression of a number of well-defined miR-34a target genes such as CDK6, SIRT1 and MET, as compared to the tRNA/MSA or vehicle treatments (Figure 4B). In addition, we compared side-by-side the effectiveness of biological and synthetic miR-34a agents in human cell line models. Interestingly, our data showed that recombinant tRNA/mir-34a was relatively more effective to suppress the proliferation of A549 and HepG2 cells and the protein levels of miR-34a target genes (e.g., CDK6, SIRT1 and MET) than the same doses of synthetic pre-miR-34a and miR-34a mimics bearing artificial modifications, as compared to corresponding controls (Figure 5A-B). These results indicate that tRNA-carried pre-miR-34a is biologically/pharmacologically active in the modulation of miR-34a target gene expression and cancer cell proliferation.

Recombinant pre-miR-34a is effective to suppress xenograft tumor progression in mouse models. We thus evaluated the therapeutic effects of tRNA/mir-34a *in vivo* using human lung carcinoma A549 and hepatic carcinoma HepG2 xenograft tumor mouse models. When A549 xenograft tumors reached ~150 mm^3 typically within 3 weeks after inoculation, we treated male nude mice intratumorally with 20 or 100 μg of *in vivo*-jetPEI-formulated tRNA/mir-34a, which would not be complicated by tissue distribution. Separate groups of animals were administered with the same doses of *in vivo*-jetPEI-formulated tRNA/MSA or only the *in vivo*-jetPEI vehicle as controls. Our data showed that, compared to the vehicle treatment or the same dose of tRNA/MSA, the higher dose (100 μg) of tRNA/mir-34a led to a complete disappearance of the A549 xenograft tumors (3 out of 6) and an overall significant repression of the outgrowth of viable tumors (Figure 6A). The same dose (100 μg) of tRNA/mir-34a also significantly suppressed the growth of HepG2-derived xenografts (Figure 6B), although to a lower degree

JPET Fast Forward. Published on May 28, 2015 as DOI: 10.1124/jpet.115.225631
This article has not been copyedited and formatted. The final version may differ from this version.

than its effects on A549 xenografts. These findings indicate that recombinant tRNA-carried pre-miR-34a is effective to control xenograft tumor progression *in vivo*.

Chimeric ncRNAs are well tolerated in mouse models. We further investigated the safety profiles of recombinant tRNA/mir-34a agents produced in *E. coli*. The Limulus Amebocyte Lysate (LAL) assay was first conducted to evaluate whether these biological ncRNAs contain significant levels of endotoxin that may cause immune response or toxicity in mammalian cells. While total RNAs isolated from *E. coli* showed variable levels of endotoxin (100-1,000 EU/μg RNA), endotoxin activities were minimal for the ncRNAs purified with FPLC (<10 EU/μg RNA) and those further processed with an endotoxin removal kit (< 3.0 EU/μg RNA). Despite the lack of an endotoxin safety standard for RNA agents and the uncertainty of whether RNAs influence (the mechanism of the) LAL assay, endotoxin activities in our purified ncRNAs measured much lower than 2,000 EU/μg DNA that is required to significantly inhibit transfection and cell proliferation (Butash et al., 2000).

After verifying that *in vivo*-jetPEI-loaded tRNA/mir-34a and tRNA/MSA were protected against degradation by serum RNases (Figure 7A), we directly assessed the effects of *in vivo*-jetPEI-formulated ncRNAs on the immune response as well as hepatic and renal functions in immunocompetent BALB/c male mouse models. The activation of immune response is often indicated by the increase of blood levels of various cytokines, among which the pro- and anti-inflammatory cytokine IL-6 is the most sensitive in response to nucleic acids (Wiggins et al., 2010). As a positive control, LPS-treated mice showed an immediate sharp surge of serum IL-6 levels in 1-6 h after injection (Figure 7B), in addition to obvious signs of stress (e.g., hunched posture and labored movement), and then fully recovered within 24 h. In contrast, serum IL-6 levels were just elevated slightly in mice in 6 h after intravenous administration of 100 μg tRNA/mir-34a or tRNA/MSA. The change was very mild as compared to the LPS treatment and it was similar to that reported for synthetic miR-34a mimics (Wiggins et al., 2010) that might not indicate an adverse drug response. Furthermore, mouse blood chemistry profiles including the levels of alanine aminotransferase (ALT), aspartate aminotransferase (AST), albumin, alkaline phosphatase (ALP), total bilirubin, blood urea nitrogen (BUN), creatinine and total protein were

not significantly altered by recombinant tRNA/mir-34a (Fig. 7C), suggesting that the biological ncRNA agents did not induce acute liver or kidney toxicity.

JPET Fast Forward. Published on May 28, 2015 as DOI: 10.1124/jpet.115.225631
This article has not been copyedited and formatted. The final version may differ from this version.

Discussion

In contrast to the large efforts to develop miRNA-based therapies, translational and clinical research is often hampered by the access to large quantities of inexpensive natural miRNA agents. Motivated by the concept of deploying biological RNA agents to perform RNA actions and the principle of "prodrug", we established a novel strategy to cost-effectively produce multi-milligrams of tRNA fusion miR-34a biological agents in one liter cultures of a common strain of *E. coli* in a research laboratory setting. The better expression of recombinant ncRNA in HST08 strain may be related to the lack of gene clusters in HST08 cells for digesting methylated DNA or a lower capacity to polyadenylate ncRNA for degradation. It is noteworthy that our strategy is different from a newly report approach to generate fully-processed siRNAs using p19-expressing bacteria (Huang et al., 2013). A high-yield accumulation of recombinant tRNA/mir-34a in bacteria (~15% of total RNAs) also facilitated the purification by anion-exchange FPLC method to a high degree (>98%) of homogeneity. In addition, we were able to characterize the primary structures and modified nucleosides of recombinant ncRNAs through LC-UV-MS analyses of hydrolysates and LC-MS/MS analyses of RNase T1-cleaved fragments. Our findings illustrate fundamental posttranscriptional modifications of the tRNA scaffold that are critical for its stability (Alexandrov et al., 2006).

Chimeric tRNA/mir-34a showed a rather surprisingly favorable stability within human carcinoma cells, suggesting that the tRNA carrier also offered a "stealth delivery" of target pre-miR-34a into human cells beyond the high-yield production of chimeric tRNA/mir-34a in bacteria. As expected, chimeric tRNA/mir-34a acted as a "prodrug" in human carcinoma cells, where pre-miR-34a was selectively processed to mature miR-34a by intrinsic miRNA processing machinery and the tRNA carrier was degraded to tRFs (Lee et al., 2009; Li et al., 2012). The 70-fold higher levels of mature miR-34a were also accompanied by 60-fold increase in miR-34a-p3 small RNA derived from pre-miR-34a. Therefore, chimeric tRNA/mir-34a may serve as an optimal carrier to assemble small RNAs of interests (Chen et al., 2015) that cannot be produced with tRNA scaffold. In addition, these results offer a good understanding of the fate of recombinant ncRNAs in human cells and the susceptibility to a few commercially-available human RNases, despite that the precise contribution of specific RNases to the metabolism and

JPET Fast Forward. Published on May 28, 2015 as DOI: 10.1124/jpet.115.225631
This article has not been copyedited and formatted. The final version may differ from this version.

pharmacokinetics of biological tRNA/mir-34a warrants further investigation. While the effects of these tRFs are unknown, the same tRFs were produced from tRNA/MSA and tRNA/mir-34a at comparable levels in human cells, supporting the validity of using tRNA/MSA expressed in the same strain of *E. coli* and purified in the same manner as a control for the assessment of bioactivities of tRNA-carried pre-miR-34a.

The functions of tRNA-carried pre-miR-34a were nicely demonstrated by the selective reduction of protein expression levels of a number of previously verified miR-34a target genes such as CDK6, MET and SIRT1 in both A549 and HepG2 cells, as compared to tRNA/MSA. These genes are critical for many cellular processes such as cell cycle and apoptosis. Therefore, the suppression of miR-34a target genes by recombinant pre-miR-34a provides a mechanistic explanation for its anti-proliferative activities. The broad anticancer activities of recombinant pre-miR-34a against various types of cancer cells are consistent with previous findings on miR-34a functions in targeting multiple oncogenes and oncogenic pathways among different types of cancer cells (Chang et al., 2007; He et al., 2007; Sun et al., 2008; Yamakuchi et al., 2008; Li et al., 2009; Liu et al., 2011; Kasinski and Slack, 2012). Meanwhile, different human carcinoma cell lines did exhibit variable sensitivities to tRNA/mir-34a, which may be due to the variability in genome and gene expression profiles as well as the apparent effects of pre-miR-34a on target gene expression in different cell lines. While we posit that the activities of tRNA-carried pre-miR-34a in the modulation of miR-34a target gene expression and cancer cell growth is attributable to the mature miR-34a selectively produced from chimeric tRNA/mir-34a, we cannot exclude the possibility that pre-miR-34a itself is responsible for some of the effects noted.

Non-small cell lung cancer A549 cells consisting of KRAS mutant, wild-type p53 and wild-type EGFR commonly found in human lung carcinomas are proper models for human lung carcinogenesis and tumor progression (Lehman et al., 1991; Nomoto et al., 2006). By contrast, the hepatocellular carcinoma (HCC) HepG2 cell line represents a pure human liver carcinoma cell line free of viral infections, is comprised of a NRAS mutant, and is often used as a HCC model (Hsu et al., 1993; Charette et al., 2010; Costantini et al., 2013). Therefore, the A549 and HepG2 cells were utilized to produce xenograft tumors in mouse models to evaluate the effectiveness of recombinant pre-miR-34a in the control of tumor growth *in vivo*. Our study

JPET Fast Forward. Published on May 28, 2015 as DOI: 10.1124/jpet.115.225631
This article has not been copyedited and formatted. The final version may differ from this version.

revealed a significant suppression of both A549 and HepG2 xenograft tumor growth by the higher dose (100 μg) of tRNA/mir-34a, compared to the vehicle treatment or the same dose of tRNA/MSA. After monitoring tumor growth for 6 weeks, our data demonstrated that tRNA/mir-34a strikingly eradicated A549 tumors (3 out of 6 mice) while it is unknown whether and when recurrence would occur. Although we did not measure the half-life of tRNA/mir-34a *in vivo*, we have demonstrated that expression levels persisted until day 6 in A549 and HepG2 cell lines after single dose transfection. Meanwhile, our data showed a much greater degree of inhibition against A549 xenografts than HepG2 by tRNA/mir-34a, which is in agreement with the efficacy of tRNA/mir-34a defined with cancer cell line models *in vitro*. While this study is limited to an intratumoral drug administration, it provides direct evidence to support the effectiveness of biological miR-34a agents *in vivo*. Nevertheless, the utility of recombinant miR-34a agents for cancer treatments should be challenged using targeted drug delivery systems and/or more clinically-relevant tumor animal models before clinical investigations.

Our study also illustrated that a relatively higher dose intravenous bolus, FPLC-purified chimeric miR-34a biological agents did not cause any stress to the mice (e.g., hunched posture and labored movement) within 48 h after drug administration or alter the liver and kidney functions which were manifested by the unchanged blood chemistry profiles. The levels of serum IL-6, the most sensitive cytokine in response to nucleic acids, were only slightly perturbed by chimeric ncRNAs as compared with the LPS treatment. The minor change in IL-6 levels caused by recombinant tRNA/mir-34 and tRNA/MSA within a short period (6 h) was actually comparable to those reported for synthetic miR-34a mimics (Wiggins et al., 2010). Due to unchanged ALT, AST, bilirubin, albumin, BUN, creatinine, and total proteins levels in tRNA/mir-34a treated mice 48 h post-injection, these findings indicate that recombinant ncRNAs are well tolerated in mouse models and do not induce any acute toxicity. Nevertheless, further studies are needed to critically define the safety profiles following chronic administration of biological ncRNAs in different species of animal models before clinical studies.

It is also noteworthy that recombinant tRNA/mir-34a, as first described in the current study, was proven to be equally or more effective than synthetic pre-miR-34a and miR-34a mimics in the regulation of target gene expression and suppression of cancer cell proliferation, compared to

corresponding controls. This might be related to the differences in their secondary structures and metabolic stabilities within the cells, and consequently the efficiencies of miRNA processing machinery and RISC complex in utilizing these agents for the regulation of target gene expression and control of cellular processes. Nevertheless, the advantages and disadvantages of using recombinant miRNA agents versus synthetic miRNAs as well as recombinant DNAs for research and therapy will be undoubtedly subjected to discussion and examination.

In conclusion, our results demonstrate that chimeric pre-miR-34a agents could be produced efficiently in a common strain of *E. coli* on a large scale. The biological tRNA/mir-34a bearing natural modifications exhibited a favorable cellular stability and was degradable by RNases. Furthermore, tRNA-carried pre-miR-34a was pharmacologically active to suppress human carcinoma cell proliferation through the regulation of miR-34a target gene expression after being selectively processed to mature miR-34a. In addition, chimeric miR-34a was effective to control xenograft tumor progression while it was well tolerated in mouse models. Our findings indicate that chimeric miRNA agents engineered in bacteria may be useful tools for the discovery and development of novel pharmacotherapies.

Authorship Contributions

Participated in research design: Yu and all other authors.

Conducted experiments: Wang, Ho, Chen, Addepalli, M.-M. Li, Wu, Jilek, Yu and Qiu.

Contributed to new reagents or analytical tools: Yu, Limbach, Li, Addepalli, and Lam.

Performed data analysis: All authors.

Wrote or contributed to the writing of the manuscript: Yu, Wang, Ho and all other authors.

W.-P. W., P.Y. H., Q.-X. C. Contributed equally to this study

References

Alexandrov, A., I. Chernyakov, W. Gu, S. L. Hiley, T. R. Hughes, E. J. Grayhack and E. M. Phizicky (2006). Rapid tRNA decay can result from lack of nonessential modifications. *Mol Cell* **21**: 87-96.

Bader, A. G. (2012). miR-34 - a microRNA replacement therapy is headed to the clinic. *Frontiers in genetics* **3**: 120.

Bi, H. C., Y. Z. Pan, J. X. Qiu, K. W. Krausz, F. Li, C. H. Johnson, C. T. Jiang, F. J. Gonzalez and A. M. Yu (2014). N-methylnicotinamide and nicotinamide N-methyltransferase are associated with microRNA-1291-altered pancreatic carcinoma cell metabolome and suppressed tumorigenesis. *Carcinogenesis* **35**: 2264-2272.

Bodeman, C. E., A. L. Dzierlenga, C. M. Tally, R. M. Mulligan, A. D. Lake, N. J. Cherrington and S. C. McKarns (2013). Differential regulation of hepatic organic cation transporter 1, organic anion-transporting polypeptide 1a4, bile-salt export pump, and multidrug resistance-associated protein 2 transporter expression in lymphocyte-deficient mice associates with interleukin-6 production. *J Pharmacol Exp Ther* **347**: 136-144.

Butash, K. A., P. Natarajan, A. Young and D. K. Fox (2000). Reexamination of the effect of endotoxin on cell proliferation and transfection efficiency. *Biotechniques* **29**: 610-614, 616, 618-619.

Chang, T. C., E. A. Wentzel, O. A. Kent, K. Ramachandran, M. Mullendore, K. H. Lee, G. Feldmann, M. Yamakuchi, M. Ferlito, C. J. Lowenstein, D. E. Arking, M. A. Beer, A. Maitra and J. T. Mendell (2007). Transactivation of miR-34a by p53 broadly influences gene expression and promotes apoptosis. *Mol Cell* **26**: 745-752.

Charette, N., C. De Saeger, V. Lannoy, Y. Horsmans, I. Leclercq and P. Starkel (2010). Salirasib inhibits the growth of hepatocarcinoma cell lines in vitro and tumor growth in vivo through ras and mTOR inhibition. *Mol Cancer* **9**: 256.

Chen, Q. X., W. P. Wang, S. Zeng, S. Urayama and A. M. Yu (2015). A general approach to high-yield biosynthesis of chimeric RNAs bearing various types of functional small RNAs for broad applications. *Nucleic Acids Res* **43**: 3857-3869.

Costantini, S., G. Di Bernardo, M. Cammarota, G. Castello and G. Colonna (2013). Gene expression signature of human HepG2 cell line. *Gene* **518**: 335-345.

Craig, V. J., A. Tzankov, M. Flori, C. A. Schmid, A. G. Bader and A. Muller (2012). Systemic microRNA-34a delivery induces apoptosis and abrogates growth of diffuse large B-cell lymphoma in vivo. *Leukemia* **26**: 2421-2424.

He, L., X. He, L. P. Lim, E. de Stanchina, Z. Xuan, Y. Liang, W. Xue, L. Zender, J. Magnus, D. Ridzon, A. L. Jackson, P. S. Linsley, C. Chen, S. W. Lowe, M. A. Cleary and G. J. Hannon (2007). A microRNA component of the p53 tumour suppressor network. *Nature* **447**: 1130-1134.

Hsu, I. C., T. Tokiwa, W. Bennett, R. A. Metcalf, J. A. Welsh, T. Sun and C. C. Harris (1993). p53 gene mutation and integrated hepatitis B viral DNA sequences in human liver cancer cell lines. *Carcinogenesis* **14**: 987-992.

Huang, L., J. Jin, P. Deighan, E. Kiner, L. McReynolds and J. Lieberman (2013). Efficient and specific gene knockdown by small interfering RNAs produced in bacteria. *Nat Biotechnol* **31**: 350-356.

Ingelman-Sundberg, M., X. B. Zhong, O. Hankinson, S. Beedanagari, A. M. Yu, L. Peng and Y. Osawa (2013). Potential role of epigenetic mechanisms in the regulation of drug metabolism and transport. *Drug Metab Dispos* **41**: 1725-1731.

Kasinski, A. L. and F. J. Slack (2011). Epigenetics and genetics. MicroRNAs en route to the clinic: progress in validating and targeting microRNAs for cancer therapy. *Nature reviews. Cancer* **11**: 849-864.

Kasinski, A. L. and F. J. Slack (2012). miRNA-34 prevents cancer initiation and progression in a therapeutically resistant K-ras and p53-induced mouse model of lung adenocarcinoma. *Cancer Res* **72**: 5576-5587.

Kelnar, K., H. J. Peltier, N. Leatherbury, J. Stoudemire and A. G. Bader (2014). Quantification of therapeutic miRNA mimics in whole blood from non-human primates. *Anal Chem* **86**: 1534-1542.

Krivos, K. L., B. Addepalli and P. A. Limbach (2011). Removal of 3'-phosphate group by bacterial alkaline phosphatase improves oligonucleotide sequence coverage of RNase digestion products analyzed by collision-induced dissociation mass spectrometry. *Rapid Commun Mass Spectrom* **25**: 3609-3616.

Lee, Y. S., Y. Shibata, A. Malhotra and A. Dutta (2009). A novel class of small RNAs: tRNA-derived RNA fragments (tRFs). *Genes Dev* **23**: 2639-2649.

Lehman, T. A., W. P. Bennett, R. A. Metcalf, J. A. Welsh, J. Ecker, R. V. Modali, S. Ullrich, J. W. Romano, E. Appella, J. R. Testa and et al. (1991). p53 mutations, ras mutations, and p53-heat shock 70 protein complexes in human lung carcinoma cell lines. *Cancer Res* **51**: 4090-4096.

Li, M. M., B. Addepalli, M. J. Tu, Q. X. Chen, W. P. Wang, P. A. Limbach, J. M. LaSalle, S. Zeng, M. Huang and A. M. Yu (2015). Chimeric miR-1291 biosynthesized efficiently in E. coli is effective to reduce target gene expression in human carcinoma cells and improve chemosensitivity. *Drug Metab Dispos*: (in press).

Li, M. M., W. P. Wang, W. J. Wu, M. Huang and A. M. Yu (2014). Rapid Production of Novel Pre-MicroRNA Agent hsa-mir-27b in Escherichia coli Using Recombinant RNA Technology for Functional Studies in Mammalian Cells. *Drug Metab Dispos* **42**: 1791-1795.

Li, Y., F. Guessous, Y. Zhang, C. Dipierro, B. Kefas, E. Johnson, L. Marcinkiewicz, J. Jiang, Y. Yang, T. D. Schmittgen, B. Lopes, D. Schiff, B. Purow and R. Abounader (2009). MicroRNA-34a inhibits glioblastoma growth by targeting multiple oncogenes. *Cancer Res* **69**: 7569-7576.

Li, Z., C. Ender, G. Meister, P. S. Moore, Y. Chang and B. John (2012). Extensive terminal and asymmetric processing of small RNAs from rRNAs, snoRNAs, snRNAs, and tRNAs. *Nucleic Acids Res* **40**: 6787-6799.

Liu, C., K. Kelnar, B. Liu, X. Chen, T. Calhoun-Davis, H. Li, L. Patrawala, H. Yan, C. Jeter, S. Honorio, J. F. Wiggins, A. G. Bader, R. Fagin, D. Brown and D. G. Tang (2011). The microRNA miR-34a inhibits prostate cancer stem cells and metastasis by directly repressing CD44. *Nat Med* **17**: 211-215.

Ma, L., J. Teruya-Feldstein and R. A. Weinberg (2007). Tumour invasion and metastasis initiated by microRNA-10b in breast cancer. *Nature* **449**: 682-688.

Nelissen, F. H., E. H. Leunissen, L. van de Laar, M. Tessari, H. A. Heus and S. S. Wijmenga (2012). Fast production of homogeneous recombinant RNA--towards large-scale production of RNA. *Nucleic Acids Res* **40**: e102.

Nomoto, K., K. Tsuta, T. Takano, T. Fukui, T. Fukui, K. Yokozawa, H. Sakamoto, T. Yoshida, A. M. Maeshima, T. Shibata, K. Furuta, Y. Ohe and Y. Matsuno (2006). Detection of EGFR mutations in archived cytologic specimens of non-small cell lung cancer using high-resolution melting analysis. *Am J Clin Pathol* **126**: 608-615.

Novoa, E. M., M. Pavon-Eternod, T. Pan and L. Ribas de Pouplana (2012). A role for tRNA modifications in genome structure and codon usage. *Cell* **149**: 202-213.

Pan, Y. Z., A. Zhou, Z. Hu and A. M. Yu (2013). Small nucleolar RNA-derived microRNA hsa-miR-1291 modulates cellular drug disposition through direct targeting of ABC transporter ABCC1. *Drug Metab Dispos* **41**: 1744-1751.

Ponchon, L., G. Beauvais, S. Nonin-Lecomte and F. Dardel (2009). A generic protocol for the expression and purification of recombinant RNA in Escherichia coli using a tRNA scaffold. *Nat Protoc* **4**: 947-959.

Ponchon, L. and F. Dardel (2007). Recombinant RNA technology: the tRNA scaffold. *Nat Methods* **4**: 571-576.

Pramanik, D., N. R. Campbell, C. Karikari, R. Chivukula, O. A. Kent, J. T. Mendell and A. Maitra (2011). Restitution of tumor suppressor microRNAs using a systemic nanovector inhibits pancreatic cancer growth in mice. *Mol Cancer Ther* **10**: 1470-1480.

Russell, S. P. and P. A. Limbach (2013). Evaluating the reproducibility of quantifying modified nucleosides from ribonucleic acids by LC-UV-MS. *J Chromatogr B Analyt Technol Biomed Life Sci* **923-924**: 74-82.

Sun, F., H. Fu, Q. Liu, Y. Tie, J. Zhu, R. Xing, Z. Sun and X. Zheng (2008). Downregulation of CCND1 and CDK6 by miR-34a induces cell cycle arrest. *FEBS Lett* **582**: 1564-1568.

Taucher, M. and K. Breuker (2010). Top-down mass spectrometry for sequencing of larger (up to 61 nt) RNA by CAD and EDD. *J Am Soc Mass Spectrom* **21**: 918-929.

Wang, Y., X. Shan, Y. Dai, L. Jiang, G. Chen, Y. Zhang, Z. Wang, L. Dong, J. Wu, G. Guo and G. Liang (2015). Curcumin analog L48H37 prevents LPS-induced TLR4 signaling pathway activation and sepsis via targeting MD2. *J Pharmacol Exp Ther*.

Welch, C., Y. Chen and R. L. Stallings (2007). MicroRNA-34a functions as a potential tumor suppressor by inducing apoptosis in neuroblastoma cells. *Oncogene* **26**: 5017-5022.

Wiggins, J. F., L. Ruffino, K. Kelnar, M. Omotola, L. Patrawala, D. Brown and A. G. Bader (2010). Development of a lung cancer therapeutic based on the tumor suppressor microRNA-34. *Cancer Res* **70**: 5923-5930.

Yamakuchi, M., M. Ferlito and C. J. Lowenstein (2008). miR-34a repression of SIRT1 regulates apoptosis. *Proc Natl Acad Sci U S A* **105**: 13421-13426.

Yao, H. W. and J. Li (2015). Epigenetic modifications in fibrotic diseases: implications for pathogenesis and pharmacological targets. *J Pharmacol Exp Ther* **352**: 2-13.

Yu, A. M. (2009). Role of microRNAs in the regulation of drug metabolism and disposition. *Expert Opin Drug Metab Toxicol* **5**: 1513-1528.

Footnotes

This project was supported in part by the National Institutes of Health National Cancer Institute [Grant 1U01CA17531]; and the National Science Foundation [Grant CHE 1212625].

W.-P. W., P.Y. H., Q.-X. C. Contributed equally to this study

Send reprint requests to: Dr. Ai-Ming Yu, Department of Biochemistry & Molecular Medicine, UC Davis School of Medicine, 2700 Stockton Boulevard, Sacramento, CA 95817, USA. Phone: 916-734-1566; Fax: 916-734-4418; E-mail: aimyu@ucdavis.edu.

Supplementary materials are available online.

JPET Fast Forward. Published on May 28, 2015 as DOI: 10.1124/jpet.115.225631
This article has not been copyedited and formatted. The final version may differ from this version.

Figure Legends

Figure 1. Production and structural characterization of recombinant tRNA/mir-34a agents. (A) The secondary structure of chimeric tRNA/mir-34a (233 nt) predicted by CentroidFold showed that the stem-loop structure of mir-34a retained within the chimeric ncRNA. The heat color gradation indicates the base-pairing probability from 0 to 1. (B) Expression of tRNA/mir-34a in various strains of *E. coli*. Among those tested, the highest levels of recombinant ncRNAs were found in HST08. (C) FPLC traces of tRNA/mir-34a and tRNA/MSA during the purification. Total RNAs were separated using anion-exchange FPLC and monitored at 260 nm. (D) HPLC analysis confirmed the high homogeneity (>98%) of purified tRNA/mir-34a and tRNA/MSA. (E) LC-MS/MS mapping/sequencing of purified tRNA/mir-34a and tRNA/MSA after the digestion with RNase T1. All posttranscriptional modifications except deoxyadenosine identified by nucleoside analysis (Supplementary Figure S1) could be mapped to RNase T1 digestion products and assigned to specific sites.

Figure 2. The tRNA-carried pre-miR-34a was selectively processed to mature miR-34a in human carcinoma cells while tRNA scaffold was degraded to tRFs, as revealed by unbiased deep sequencing studies. Mature miR-34a levels were over 70-fold higher in A549 cells treated with 5 nM tRNA/mir-34a, as compared to cells treated with the control tRNA/MSA (A) or vehicle (B). This was associated with a 60- to 65-fold increase in the numbers of reads of 15-nt miR-34a-p3 fragment (5'-CACGUUGUGGGGCCC-3'). In contrast, changes in other miRNAs were small or insignificant (Supplementary Table 1 and 2), except several undefined small RNAs (e.g., hsa-mir-7641-1-p5_1ss6TC). Values are mean ± SD of triplicate treatments that were sequenced separately. (C) Mapping major tRFs derived from tRNA/mir-34a and tRNA/MSA in A549 cells. Other low-abundance tRFs are provided in Supplementary Table 4.

Figure 3. Cellular stability and RNase susceptibility of chimeric tRNA/mir-34a. (A) Chimeric tRNA/mir-34a was processed to mature miR-34a in various types of human carcinoma cells, as determined by selective stem-loop RT-qPCR analyses. Values are mean ± SD of triplicate treatments. (B) The levels of chimeric ncRNA (tRNA/mir-34a or tRNA/MSA), pre-miRNA mir-34a, and mature miRNA miR-34a were increased in a dose dependent manner ($P <$

0.001, one-way ANOVA) in A549 cells at 24 h after transfection with 1, 5 or 25 nM of FPLC-purified tRNA/mir-34a or tRNA/MSA. Note that mir-34a and miR-34a levels were only elevated in cells treated with tRNA/mir-34a. (C) Chimeric ncRNA (tRNA/mir-34a or tRNA/MSA; 5 nM) exhibited a good stability in A549 cells. Note that change in mature miR-34a levels was dependent upon tRNA/mir-34a treatment. (D) Chimeric tRNA/mir-34a and the tRNA/MSA were susceptible to a number of human RNases including RNase A, angiogenin and Dicer. RNase digestions were analyzed with 8% Urea PAGE.

Figure 4. Recombinant mir-34a was biologically/pharmacologically active in suppressing cancer cell proliferation and target gene expression. (A) tRNA/mir-34a inhibited the growth of human carcinoma A549 and HepG2 cells in a dose dependent manner and to much greater degrees than the control tRNA/MSA ($P < 0.001$, two-way ANOVA). Antiproliferative activities against H460 and Huh-7 cells are shown in Supplementary Figure S3, and the estimated ED50 and Hill Slope values are provided in Table 1. Cell viability was determined using MTT assay at 72 h post-transfection. Values are mean ± SD of triplicate cultures. (B) Compared to the control tRNA/MSA, recombinant tRNA/mir-34a sharply reduced the protein levels of a number of miR-34a target genes including CDK6, MET and SIRT1 in A549 and HepG2 cells. Western blots were conducted using protein selective antibodies. GAPDH was used as a loading control.

Figure 5. Recombinant mir-34a was equally or more effective than synthetic miR-34a mimics to reduce human carcinoma cell proliferation and target gene expression. (A) The effects of 5 nM biologic tRNA/mir-34a, and synthetic miR-34a precursor and mimics on the growth of A549 and HepG2 carcinoma cells. Cell viability was determined using MTT assay at 72 h post-transfection. Values are mean ± SD of triplicate treatments. *$P < 0.05$, compared to corresponding control. (B) The effects of 25 nM recombinant mir-34a and synthetic miR-34a mimics on the protein levels of miR-34a target genes CDK6, MET, and SIRT1 in A549 and HepG2 carcinoma cells, as determined by Western blots at 72 h post-transfection.

Figure 6. Recombinant mir-34a was effective to control xenograft tumor progression in mouse models. (A) Compared to the same dose of tRNA/MSA or vehicle control, tRNA/mir-34a (100 μg) significantly ($P < 0.001$, unpaired t test) suppressed the growth of A549 xenograft

tumors. Note that the tumors in three mice completely disappeared after the treatment with 100 μg of tRNA/mir-34a. (B) Growth of HepG2 xenograft tumors were also significantly ($P < 0.01$, unpaired t test) suppressed by the 100 μg dose tRNA/mir-34a treatment, as compared with the same dose of tRNA/MSA or vehicle. FPLC-purified ncRNAs were administered intratumorally every the other day for three times. Values are mean ± SD (N = 6 per group for A549 xenografts; N = 4 per group for HepG2 xenografts). Separate groups of mice (N = 4) were treated with vehicle as additional controls.

Figure 7. Biologic ncRNAs were well tolerated in mouse models. (A) *In vivo*-jetPEI-loaded ncRNAs were protected against the degradation by serum RNases. (B) Compared with vehicle control treatment, *in vivo*-jetPEI formulated recombinant ncRNAs (100 μg, i.v.) did not cause significant change in mouse serum IL-6 levels while LPS did (two-way ANOVA with Bonferroni post-tests). (C) Recombinant ncRNAs (100 μg, i.v.) had no significant influence on blood chemistry profiles including alanine aminotransferase (ALT), aspartate aminotransferase (AST), blood urea nitrogen (BUN), alkaline phosphatase (ALP), creatinine, total bilirubin, albumin and total protein. The gray-shaded area indicates the guideline ranges reported by the Comparative Pathology Laboratory at UC Davis. Values are mean ± SD (N = 3-4 mice per time point and treatment).

JPET Fast Forward. Published on May 28, 2015 as DOI: 10.1124/jpet.115.225631
This article has not been copyedited and formatted. The final version may differ from this version.

Table 1. Estimated EC50 and Hill slope values for the suppression of human carcinoma cell proliferation by recombinant tRNA/mir-34a and control tRNA/MSA (Goodness of Fit R^2 > 0.75). "Not fitted" means that the Goodness of Fit is less than 0.50. *Significantly ($P < 0.05$) different from the control tRNA/MSA in the same cell line.

Cell lines	EC50 (nM)		Hill slope	
	tRNA/MSA	tRNA/mir-34a	tRNA/MSA	tRNA/mir-34a
A549	Not fitted	7.80 ± 1.19	Not fitted	-2.18 ± 0.59
H460	158 ± 1	5.72 ± 1.09*	-0.86 ± 0.20	-1.32 ± 0.14*
HepG2	87.9 ± 1.1	4.75 ± 1.21*	-1.74 ± 0.40	-0.96 ± 0.18*
Huh-7	Not fitted	11.1 ± 1.2	Not fitted	-0.66 ± 0.07

Fig. 1

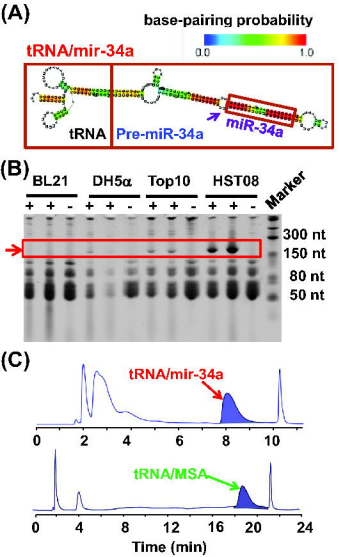

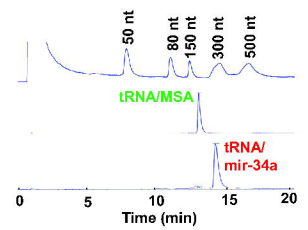

(E)

Oligo-Nucleotide	m/z (Da/e)	Location in tRNA/MSA	Location in tRNA/mir-34a
CUACG	763.1	C3:G7	C3:G7
[s4U]AG	933.1	[s4U]8:G10	[s4U]8:G10
CUCAG	763.1	C11:G15	C11:G15
CUCA[Gm]UUG	1248.7	C11:G18	C11:G18
[D][D]AG	613.4	[D]20:G23	[D]20:G23
CAG	916.2	C26:G28	C26:G28
UAAUUUACG	1398.7	U37:G45	U37:G45
[m7G][acp3U]CACAG	1157.7	[m7G]77:G83	[m7G]:G203
[m5U]ψCG	1213.1	[m5U]85:G88	[m5U]211:G214
AAUCCCG	1080.1	A89:G95	A215:G221
CCACCA	907.5	C102:A107	C228:A233
UUUCUUUG	1211.1		U73:G80
CAAUCAG	1092.1		C121:G127
UAUACUG	1081.4		U132:G138
CCCAAG	927.3		C165:G170

Fig. 2

(C)

5'-GGCUACGUAGCUCAGUUGGUUAGAGCAGCGGCCGAGU.....CACAAGGUUCGAAUCCCGUCGUAGCCACCA-3'

tRNA/MSA (reads)	tRNA/mir-34a (reads)	
16,450±2,261	13,696±2,089	AAUCCCGUCGUAGCCACCA
16,207±6,284	10,677±1,368	AGUUGGUUAGAGCAGCGGCC
14,710±5,849	8,064±2,595	GUUCGAAUCCCGUCGUAGCC
12,892±2,656	2,700±1,157	CCACAGGUUCGAAUCCCGUCGUAGCCACCA
12,849±4,739	11,836±1,044	AAUCCCGUCGUAGCC
10,260±2,123	1,748± 448	UUCGAAUCCCGUCGUAGCCACC
9,028±1,287	5,577±1,316	AGUUGGUUAGAGCAGCGGCCG
8,942±4,345	3,351± 451	AGUUGGUUAGAGCAGCGGC
6,939± 920	6,670± 768	AUCCCGUCGUAGCCACCA
6,276±1,103	1,980± 881	ACAGGUUCGAAUCCCGUCGUAGCCACCA

Fig. 3

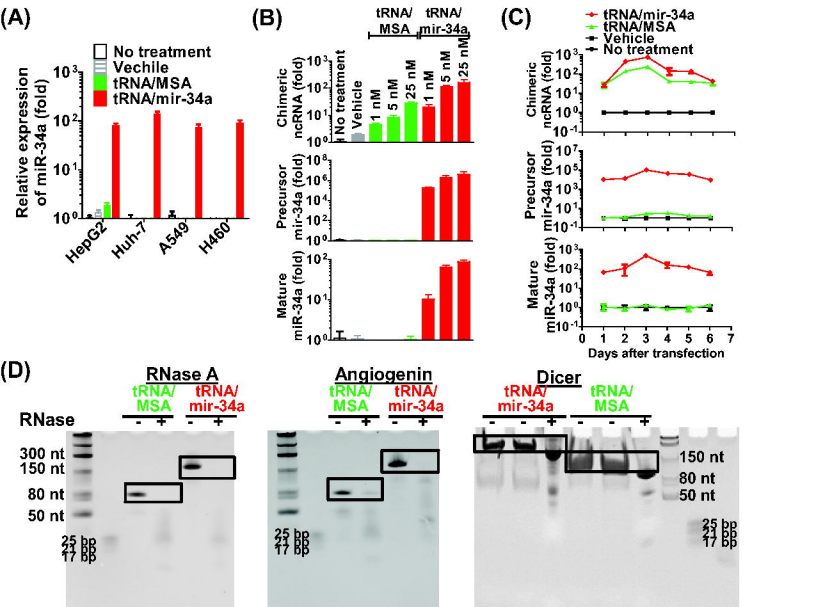
(A)
No treatment
Vechile
tRNA/MSA
tRNA/mir-34a
Relative expression of miR-34a (fold)
HepG2
Huh-7
A549
H460
(B)
tRNA/MSA
tRNA/mir-34a
No treatment
Vehicle
1 nM
5 nM
25 nM
1 nM
5 nM
25 nM
Chimeric ncRNA (fold)
Precursor miR-34a (fold)
Mature miR-34a (fold)
(C)
tRNA/mir-34a
tRNA/MSA
Vehicle
No treatment
Chimeric ncRNA (fold)
Precursor miR-34a (fold)
Mature miR-34a (fold)
Days after transfection
(D)
RNase A
Angiogenin
Dicer
tRNA/MSA
tRNA/mir-34a
RNase
300 nt
150 nt
80 nt
50 nt
25 bp
21 bp
17 bp

Fig. 4

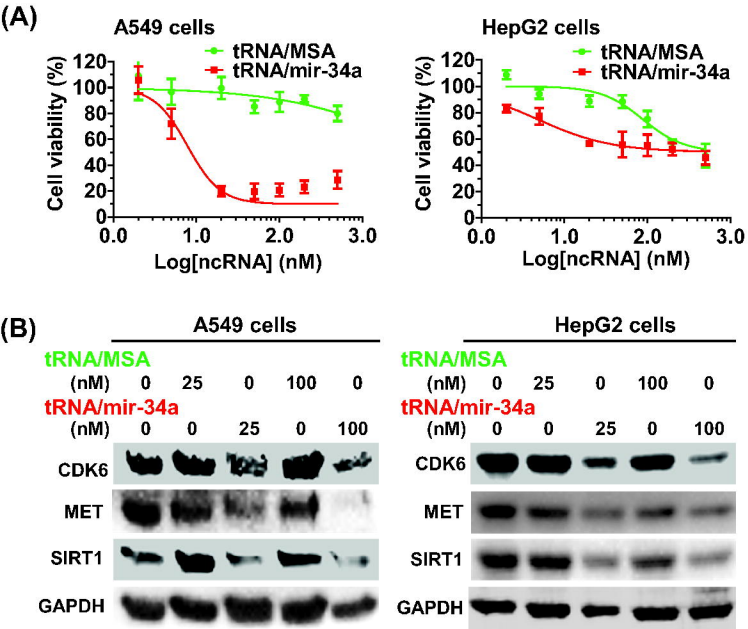
(A)
A549 cells
tRNA/MSA
tRNA/mir-34a
Cell viability (%)
Log[ncRNA] (nM)
HepG2 cells
tRNA/MSA
tRNA/mir-34a
Cell viability (%)
Log[ncRNA] (nM)
(B)
A549 cells
HepG2 cells
tRNA/MSA
(nM) 0 25 0 100 0
tRNA/mir-34a
(nM) 0 0 25 0 100
CDK6
MET
SIRT1
GAPDH

Fig. 5

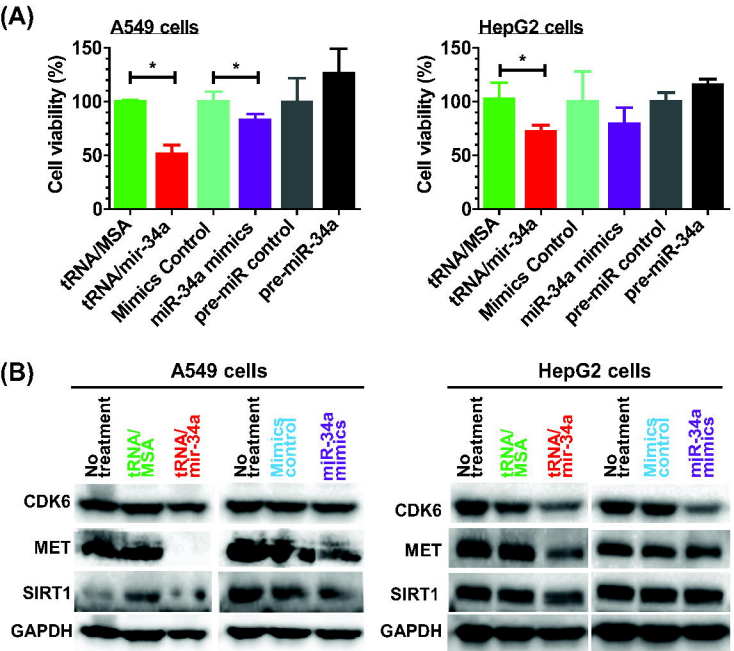
(A)
A549 cells
Cell viability (%)
150
100
50
0
*
*
tRNA/MSA
tRNA/mir-34a
Mimics Control
miR-34a mimics
pre-miR control
pre-miR-34a
HepG2 cells
Cell viability (%)
150
100
50
0
*
tRNA/MSA
tRNA/mir-34a
Mimics Control
miR-34a mimics
pre-miR control
pre-miR-34a
(B)
A549 cells
No treatment
tRNA/ MSA
tRNA/ mir-34a
No treatment
Mimics control
miR-34a mimics
CDK6
MET
SIRT1
GAPDH
HepG2 cells
No treatment
tRNA/ MSA
tRNA/ mir-34a
No treatment
Mimics control
miR-34a mimics
CDK6
MET
SIRT1
GAPDH

Fig. 6

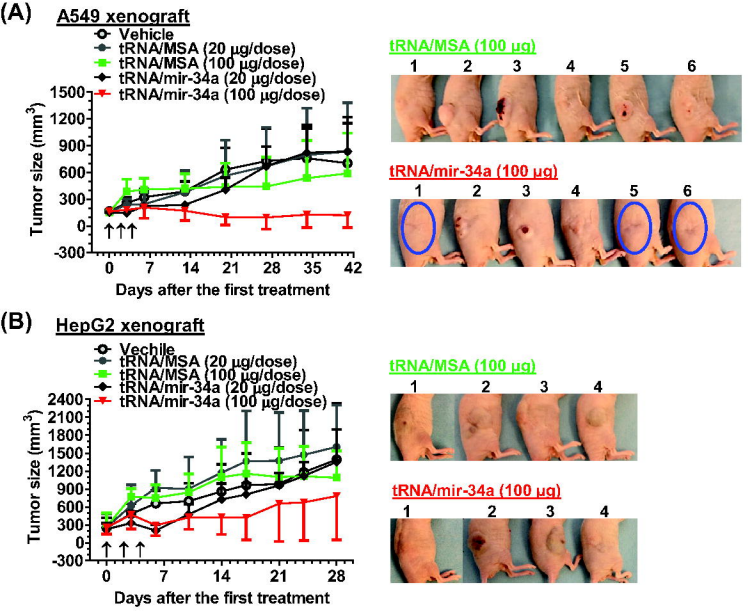
(A)
A549 xenograft
Vehicle
tRNA/MSA (20 μg/dose)
tRNA/MSA (100 μg/dose)
tRNA/mir-34a (20 μg/dose)
tRNA/mir-34a (100 μg/dose)
Tumor size (mm3)
1500
1200
900
600
300
0
-300
0
7
14
21
28
35
42
Days after the first treatment
tRNA/MSA (100 μg)
1
2
3
4
5
6
tRNA/mir-34a (100 μg)
1
2
3
4
5
6
(B)
HepG2 xenograft
Vechile
tRNA/MSA (20 μg/dose)
tRNA/MSA (100 μg/dose)
tRNA/mir-34a (20 μg/dose)
tRNA/mir-34a (100 μg/dose)
Tumor size (mm3)
2400
2100
1800
1500
1200
900
600
300
0
-300
0
7
14
21
28
Days after the first treatment
tRNA/MSA (100 μg)
1
2
3
4
tRNA/mir-34a (100 μg)
1
2
3
4

Fig. 7

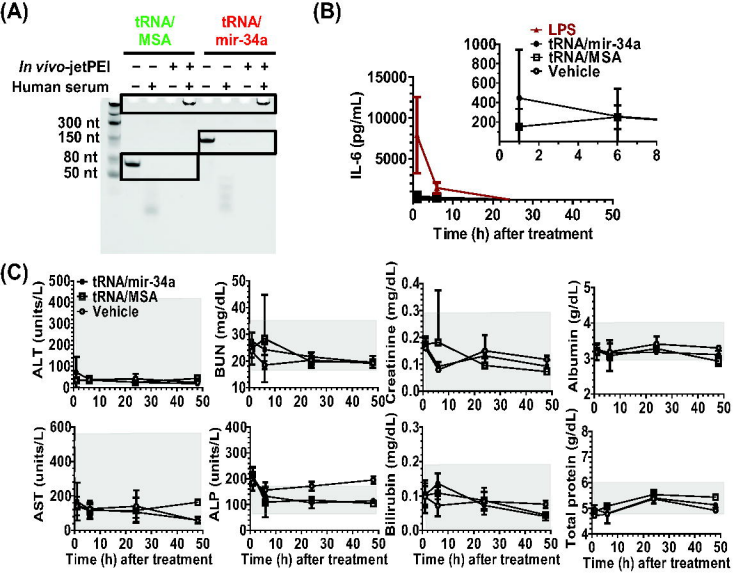
(A)
tRNA/ MSA
tRNA/ mir-34a
In vivo-jetPEI
Human serum
300 nt
150 nt
80 nt
50 nt
(B)
LPS
tRNA/mir-34a
tRNA/MSA
Vehicle
IL-6 (pg/mL)
Time (h) after treatment
(C)
tRNA/mir-34a
tRNA/MSA
Vehicle
ALT (units/L)
BUN (mg/dL)
Creatinine (mg/dL)
Albumin (g/dL)
AST (units/L)
ALP (units/L)
Bilirubin (mg/dL)
Total protein (g/dL)
Time (h) after treatment